Available online at www.sciencedirect.com

ScienceDirect

Procedia Technology 15 (2014) 268 – 277

Procedia Technology

2nd International Conference on System-integrated Intelligence: Challenges for Product and Production Engineering

A cascaded approach for quadrotor's attitude estimation

Bara J. Emran, Muhannad Al-Omari, Mamoun F. Abdel-Hafez*, Mohammad A. Jaradat

Mechanical Engineering Department, American University of Sharjah, P.O. Box 26666, Sharjah, UAE

Abstract

This paper presents a new methodology to estimate the orientation of a quadrotor using single low cost IMU sensor. The proposed solution uses two extended Kalman filters (EKF) along with a Direction Cosine Matrix (DCM) algorithm. An EKF is used to filter the noise signal of the angular rates measured by a 3-axis gyroscope sensor. Subsequently, a DCM algorithm uses the filtered gyro signal along with the reading from a 3-axis accelerometer and a 3-axis magnetometer sensor to compute the Euler angles. Finally, another EKF is presented to improve the estimation of the Euler angles. A complete simulation platform was developed using MatLab software to test the performance of the proposed method and compare it with two alternative methods.

Peer-review under responsibility of the Organizing Committee of SysInt 2014.

Keywords: extended Kalman filter; EKF; quadrotor, direction cosine matrix algorithm; DCM; attitude estimation

1. Introduction

In the last decade, unmanned aerial vehicles (UAV) have received considerable attention covering a wide area of applications for both indoor and outdoor navigation tasks. Due to several key advantages, quadrotor has recently been drawing a major focus of research attention over other UAVs for indoor navigation applications. The quadrotor

* Corresponding author. Tel.: +(971) 6 515 2910; fax: +(971) 6 515 2979.
E-mail address: mabdelhafez@aus.edu.

Peer-review under responsibility of the Organizing Committee of SysInt 2014.
doi:10.1016/j.protcy.2014.09.080

design and technology have been significantly enhanced in the last few years. These enhancements make it able to achieve a high dynamical maneuverability. It is also recognized for its compact size, simple mechanical system, vertical takeoff/landing ability, improved payload, longer flight time, and variety of onboard sensors. These key advantages make the quadrotor suitable for fast maneuvering within complex indoor environments occupied with different obstacles, and for accomplishing certain navigation tasks.

However, fast and accurate estimates of the vehicle's state are needed in order to achieve high maneuverability within a bounded indoor environment. The attitude and attitude rates of the quadrotor are especially important for stabilizing the quadrotor within complex indoor environments. Therefore, the quadrotor is installed with different sensors to measure its attitude and altitude within indoor and outdoor environments. Among these sensors are inertial measurement unit (IMU) with three mutually-orthogonal accelerometer sensors and gyroscope sensors, global positioning system (GPS) receivers, sonars, barometric systems, camera vision systems, optical flow sensors, and a laser/infrared rangefinder and depth systems.

There are many techniques and algorithms that have been introduced recently to improve the accuracy of the Inertial Navigation Systems (INS). An Implementation and comparisons between several algorithms for step detection, stride length, heading and position estimation is introduced for low-performance Micro-Electro-Mechanical (MEMS) inertial sensors while under classical coning motion in [1]. However in [2], an enhance INS solutions were proposed by estimating the measurement noise statistics. Also, an Error modification and an accuracy enhancement have been done using a fusion scheme of two-step adaptive robust filtering based on the observability of the parameters in [3]. In [4], the author made an improvement in the integrated navigation system by using a probabilistic bias fault detection method. Though in [5], an intelligent fusion method that takes into account the possible, varying, delay between INS and GPS measurements was proposed. In [6], the author shows a reduced INS to improve the system performance for a land vehicle aided by GPS single point positioning solution and the velocity derived from GPS carrier phase measurements.

The DCM algorithm is commonly used for estimate the Euler angles. The DCM algorithm improves the estimation of the Euler angles and minimizes its error by using the reading from the gyro sensor along with readings from the accelerometer and the magnetometer. Different methods and techniques have been developed using the DCM algorithm. A direct complementary filter is formulated as deterministic observer kinematics are imposed directly on a 3D special orthogonal group and driven by reconstructed attitude and angular velocity measurements in [7]. In [8], a nonlinear complementary filter that combines gyro meter output for high frequency estimation with integrated accelerometer output for low frequency attitude estimation is proposed. Also, [9] introduces a complementary filter that evolves on the Special Euclidean Group SE (3) using a combination of low-cost INS and a vision sensor. The author In [10] proposes a coupled non-linear attitude estimation and control design for the attitude stabilization of low-cost aerial robotic vehicles.

A new approach for estimating the orientation of a quadrotor using a single low-cost IMU sensor is presented in this paper. The proposed hybrid solution contains two extended Kalman filters (EKF) along with a Direction Cosine Matrix (DCM) algorithm. An EKF utilizes the dynamics of the quadrotor to filter the noise on the body frame angular rates measured by the three-axis gyroscope sensor. Next, a DCM algorithm uses the filtered gyro signal along with the reading from a three-axis accelerometer and magnetometer sensor to estimate the Euler angles. In the final step, an additional EKF is presented to enhance the final estimates of the Euler angles.

The layout of this paper is as follows. In Section 2, the quadrotor modeling is discussed. The development of the proposed hybrid approach is demonstrated in Sections 3 and 4. Section 5 presents the performance of the proposed hybrid approach. Finally, conclusion remarks are made in Section 6.

2. Quadrotor Modeling

2.1. Basic Knowledge*:*

To describe the motion of quadrotor, it is necessary to define a suitable coordinate system. The body-frame is a right-hand reference denoted by x_B, y_B, z_B and it is attached to the centre of gravity of the quadrotor. The earth-fixed frame is an inertial right-hand reference denoted by x_E, y_E, z_E. The Euler angles Θ^E are denoted by φ,θ,ψ they

represent the attitude of the quadrotor and are defined by the orientation of B-frame with respect to the E-frame. A rotation matrix is needed to map the orientation of a vector from B-frame to E-frame and vice versa. The rotation matrix is described in (1). Figure 1 describes the reference frames used in this paper.

$$R = R_z(\psi)R_y(\theta)R_x(\phi) \tag{1}$$

where, $R_z(\psi)$ denotes the rotation about the z-axis with the angle ψ, $R_y(\theta)$ denotes the rotation around the y-axis with with the angle θ, and $R_x(\phi)$ denotes the rotation around the x-axis with the angle ϕ.

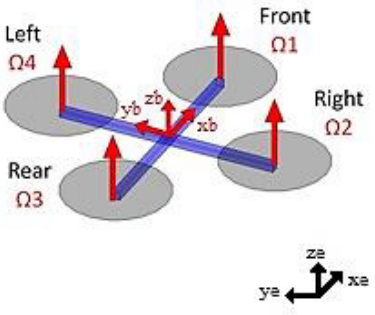

Fig. 1. Body frame and earth fixed frame.

2.2. Dynamic Model

The quadrotor's dynamical model includes the nonlinear equations of motion, along with the actuators dynamics and saturation limits [11]-**Error! Reference source not found.**. The model that was used in this paper is represented in (2).

$$\begin{aligned}
\ddot{x} &= (sin\psi\ sin\emptyset + cos\psi\ sin\theta\ cos\emptyset)\ \frac{U1}{m} \\
\ddot{y} &= (-cos\psi\ sin\emptyset + sin\psi\ sin\theta\ cos\emptyset)\ \frac{U1}{m} \\
\ddot{z} &= -g + (cos\theta\ cos\emptyset)\frac{U1}{m} \\
\dot{p} &= \frac{I_{YY} - I_{ZZ}}{I_{XX}}\ q\ r + \frac{U2}{I_{XX}} \\
\dot{q} &= \frac{I_{ZZ} - I_{XX}}{I_{YY}}\ p\ r + \frac{U3}{I_{YY}} \\
\dot{r} &= \frac{I_{XX} - I_{YY}}{I_{ZZ}}\ q\ p + \frac{U4}{I_{ZZ}}
\end{aligned} \tag{2}$$

where X, Y and Z represents the position of the center of gravity of the quadrotor with respect to the inertial frame. $p, q\ and\ r$ are the angular rates with respect to the body frame, m is the quadrotor's mass, I_{XX}, I_{YY}, I_{ZZ} are the moments of inertia along X,Y and Z axes respectively. U_1 is throttle force, U_2, U_3, U_4 are roll, pitch and yaw moments respectively.

The actuator's dynamics are governed by the following equations.

$$U_1 = b(\Omega_1^2 + \Omega_2^2 + \Omega_3^2 + \Omega_4^2)$$
$$U_2 = bl(-\Omega_2^2 + \Omega_4^2) \quad (3)$$
$$U_3 = bl(-\Omega_1^2 + \Omega_3^2)$$
$$U_4 = d(-\Omega_1^2 + \Omega_2^2 - \Omega_3^2 + \Omega_4^2)$$

where Ω_i is the propeller's speed of motor i, b is the thrust factor, d is the drag factor and l is the radius of the quadrotor.

3. Direction Cosine Matrix (DCM)

The DCM is a method used to compute the Euler angles using information from the rate gyros, accelerometers, magnetic compass and/or GPS. Integrating the gyroscope sensor's readings is the primary source of orientation information to obtain the Euler angles. The integration process will introduce numerical errors which will violate the orthogonality constraints in the direction cosine matrix. Also, the gyro drift and gyro offset will cause a gradual accumulation of errors in the Euler angles values. To solve this problem, a renormalization process in the direction cosine matrix has been used to satisfy the orthogonality constraints. In addition, two reference vectors with a PI control are used to minimize the offsets and the drifts in the gyro's readings.

Due to the rotation of body frame with respect to the navigation frame, the update of the attitude DCM can be found using the following differential equation

$$\frac{dr(t)}{dt} = \omega(t) \times r(t) \quad (4)$$

where $r(t)$ is a vector fixed in the body frame and $\omega(t)$ is the vector rotational rate of the body frame. Using the dynamic equation above, the relation between the rotation matrix and the angular rate can be expressed in a matrix form as follows:

$$R(t+dt) = R(t) + R(t)Skew(d\theta)$$
$$R(t+dt) = R(t)\begin{bmatrix} 1 & -d\theta_z & d\theta_y \\ d\theta_z & 1 & -d\theta_x \\ -d\theta_y & d\theta_x & 1 \end{bmatrix} \quad (5)$$

where:

$$d\theta_x = \omega_x dt, \qquad d\theta_y = \omega_y dt, \qquad d\theta_z = \omega_z dt \quad (6)$$

to enforce the orthogonality condition on the rotation matrix. With X and Y being columns of R(t) the orthogonal error between the two vectors is found as follows:

$$error = X^T Y = [r_{xx} \quad r_{xy} \quad r_{xz}]\begin{bmatrix} r_{yx} \\ r_{yy} \\ r_{yz} \end{bmatrix} \quad (7)$$

Then, by rotating each vector, in the opposite direction, by half of the error will ensure the orthogonally in the rotation matrix:

$$X_{Orth} = \begin{bmatrix} r_{xx} \\ r_{xy} \\ r_{xz} \end{bmatrix}_{Orth} = X - \frac{error}{2} Y$$
$$Y_{Orth} = \begin{bmatrix} r_{yx} \\ r_{yy} \\ r_{yz} \end{bmatrix}_{Orth} = Y - \frac{error}{2} X \quad (8)$$

Next, a cross product between the orthogonal vectors X and Y is done to ensure the orthogonally in the Z-vector:

$$Z_{Orth} = \begin{bmatrix} r_{zx} \\ r_{zy} \\ r_{zz} \end{bmatrix}_{Orth} = X_{Orth} \times Y_{Orth} \quad (9)$$

By scaling each vector (7),(8) and (9), we can assure the normalization conditions of the rotation matrix. The rows of the rotation matrix are enforced to have a magnitude of 1.0 as:

$$X_{Norm} = \frac{X_{Orth}}{\|X_{Orth}\|}, \qquad Y_{Norm} = \frac{Y_{Orth}}{\|Y_{Orth}\|}, \qquad Z_{Norm} = \frac{Z_{Orth}}{\|Z_{Orth}\|} \quad (10)$$

The GPS provides a drift-free reference vector for the yaw orientation (heading angle). As a result, it has been used as a reference for the horizontal projection of the X axis (roll axis). Figure 3 along with equations (11 - 13) explain how the yaw correction vector has been computed, where (X_{bMagn}) denotes the reference vector obtained from the measured magnetometer's yaw angle (ψ) is the estimated yaw, (ψ_m) is the magnetometer's measured yaw, [x_e ,y_e ,z_e] is the earth frame, [x_b ,y_b ,z_b] is the body frame and X_{bp} is the projection of x_b on the xy plane. The coordinated of the reference vector, X_{bMagn} in the earth frame are first obtained from the following equations

$$Y_{b_{Magn}} = sin(\psi_m)$$
$$X_{b_{Magn}} = cos(\psi_m) \quad (11)$$

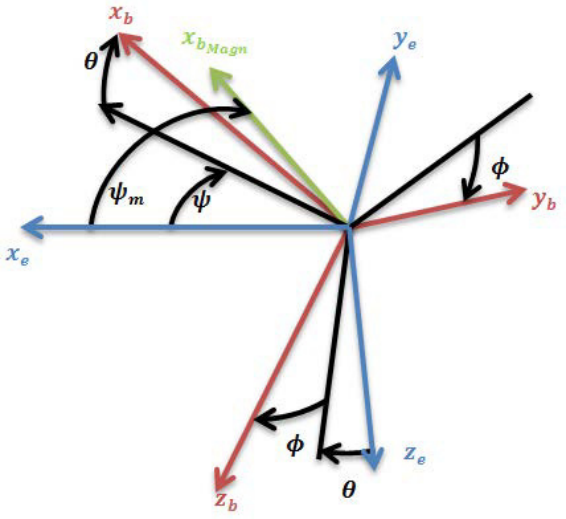

Fig. 2. Yaw correction.

The yaw corrections (rotation around the earth z-axis) is then obtained in the earth frame by the negative of the cross product between the first two entries of the X_b and with the x and y components of X_{bMagn} as:

$$\psi_{\boldsymbol{CorrG}} = r_{xx}\, Y_{b_{Magn}} - r_{yx}\, X_{b_{Magn}} \tag{12}$$

The rotational angular error between the X_{bMagn} vector and the projection on the horizontal plane of the roll axis of the IMU is an indication of the amount of drift. The yaw angle correction angle is obtained in body frame by multiplying the result of equation (13) by the z-row of the rotation matrix as:

$$\psi_{\boldsymbol{CorrB}} = \psi_{\boldsymbol{CorrG}} \begin{bmatrix} r_{zx} \\ r_{zy} \\ r_{zz} \end{bmatrix} \tag{13}$$

3.1. Gravity Acceleration Reference:

The accelerometer readings can be considered as a direct measurement of the orientation while a gyroscope measures the time rate change of the orientation. As a result, it has been used as a reference vector for the Z-axis acceleration.

Given that the accelerometer measures specific force, the gravity acceleration reference vector can be calculated using the following equation:

$$\boldsymbol{g}_{ref} = BodyAcceleration - Acceleromter \tag{14}$$

By assuming small body acceleration in case of hovering situation, a simplification could be done in (15). The acceleromter will be assumed to measure only the gravity acceleration reference vector.

$$Acceleromter \approx -\boldsymbol{g}_{ref} \tag{15}$$

The cross product between the normalized Z-vector in (10) and the gravity acceleration reference vector (16) produces the roll-pitch rotational correction vector in the reference body frame:

$$\phi\theta_{\boldsymbol{Corr}} = \begin{bmatrix} r_{zx} \\ r_{zy} \\ r_{zz} \end{bmatrix} \times (-\boldsymbol{g}_{ref}) \tag{16}$$

3.2. PI controller

The total correction vector is obtained by a weighted sum of the rotational drift correction vectors in (11) and (17) as:

$$T_{Corr} = W_1\, \phi\theta_{Corr} + W_2\, \psi_{CorrB} \tag{17}$$

Then the total Correction vector T_{Corr} is fed to a PI controller as follows:

$$\begin{gathered} \omega_{P_{Corr}} = K_P\, T_{Corr} \\ \omega_{I_{Corr}} = \omega_{I_{Corr}} + K_I\, dt\, (T_{Corr}) \\ \omega_{Corr} = \omega_{P_{Corr}} + \omega_{I_{Corr}} \end{gathered} \tag{18}$$

where K_p is the proportional gain and K_I is the integration gain. Next, the Correction vector is added to the gyro vector to produce a corrected gyro vector.

$$\omega = \omega_{gyro} + \omega_{Corr} \tag{19}$$

Where ω_{Gyro} is the three-axis gyro measurement vector and ω_{Corr} is the gyro offset and drift correction vector.

4. Extended Kalman Filter (EKF)

The Kalman filter (KF) is a linear, discrete time, finite dimensional time-varying system that evaluates the state estimate that *minimizes* the mean-square error. In a situation where either the system state dynamics or the observation dynamics are nonlinear, the probability density functions conditions that provide the minimum mean-square estimate are no longer Gaussian. An approach to solve the problem in the frame of linear filters is the EKF [16]. The EKF implements a KF for a system dynamics that results from the linearization of the original non-linear dynamic equation around the state estimates.

Consider the *non*-linear dynamics:

$$\begin{aligned} \dot{\boldsymbol{x}}(t) &= f\big(\boldsymbol{x}(t), \boldsymbol{u}(t)\big) + \boldsymbol{\Gamma v}(t) \\ \boldsymbol{z}(t) &= h\big(\boldsymbol{x}(t)\big) + \boldsymbol{w}(t) \end{aligned} \tag{20}$$

v(k) and *w(k)* are white Gaussian, independent random processes with zero mean and corresponding covariance matrices represented as:

$$\begin{aligned} \boldsymbol{v}(t) &\sim N\big(0, \boldsymbol{Q}(t)\big) \\ \boldsymbol{w}(t) &\sim N\big(0, \boldsymbol{R}(t)\big) \end{aligned} \tag{21}$$

In this paper the proposed solution was developed using two EKF which are the “Rate EKF” and “Euler EKF”. These two filters are described below.

4.1. Rate EKF

The rate extended Kalman filter is used to filter the gyroscope sensors measurement. The rate EKF takes the rate gyro sensor’s readings as the measurement vector and the actuator commands as the input vector. Then by using the nonlinear model of the quadrotor (2) it filters the measurements of the gyroscope. The state matrices of the rate EKF are shown below:

$$\begin{aligned} \dot{\boldsymbol{x}}_1(t) &= f_1\big(\boldsymbol{x}(t)\big) + \boldsymbol{B}_1\boldsymbol{u}_1(t) + \boldsymbol{\Gamma} v(t) \\ \boldsymbol{z}_1(t) &= \boldsymbol{H}_1\boldsymbol{x}(t) + w(t) \end{aligned} \tag{22}$$

where:

$$f_1(t) = \begin{bmatrix} \frac{I_{YY} - I_{ZZ}}{I_{XX}}\, q\, r \\ \frac{I_{ZZ} - I_{XX}}{I_{YY}}\, p\, r \\ \frac{I_{XX} - I_{YY}}{I_{ZZ}}\, q\, p \end{bmatrix},\ \boldsymbol{B}_1 = \begin{bmatrix} \frac{1}{I_{xx}} & 0 & 0 \\ 0 & \frac{1}{I_{yy}} & 0 \\ 0 & 0 & \frac{1}{I_{zz}} \end{bmatrix},\ \boldsymbol{H} = I_{3x3} \tag{23}$$

The state variables are chosen as:

$$x_1 = [p \quad q \quad r] \tag{24}$$

The measurements are:

$$z_1 = [p \quad q \quad r] \tag{25}$$

Linearizing the function (f_1) using (31):

$$\boldsymbol{F}_1 = \begin{bmatrix} 0 & \alpha_1 r & \alpha_1 q \\ \alpha_2 r & 0 & \alpha_2 p \\ 0 & 0 & 0 \end{bmatrix} \tag{26}$$

where $\alpha_1 = -0.65,\ \alpha_2 = 0.6889$.

The result of the rate EKF in filtering the gyro's readings is shown in Figure 3. In each sub-figure, the truth angular rate, measured angular rate and filtered angular rate are shown. It can be seen that the EKF filter reduces the noise in the measured angular rates along the three body axes.

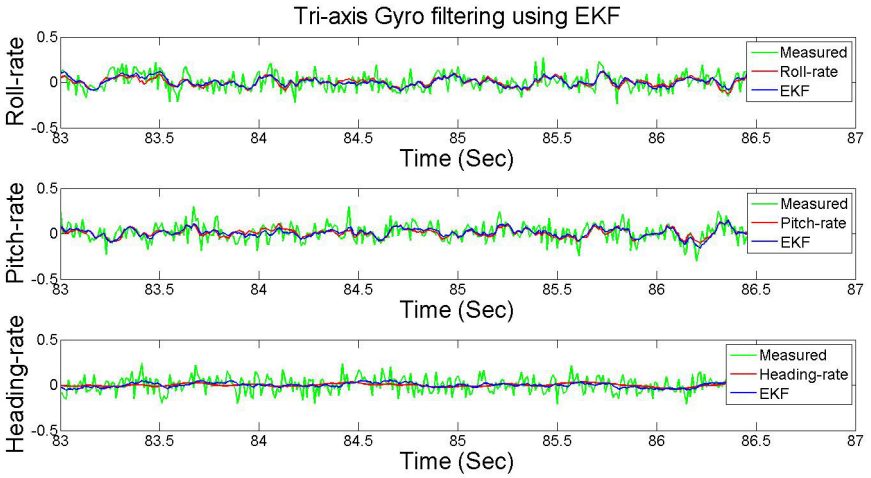

Fig. 3. Rate EKF results in filtering the gyroscope readings

4.2. Euler EKF

The Euler EKF is used to improve the estimate of the Euler angles. The Euler EKF takes the filtered angular rate as the input vector. On the other hand, the Euler angles computed using the DCM algorithm are taken as the measurement vector. With the Euler angle state vector given as

$$\boldsymbol{x}_2 = [\phi \quad \theta \quad \psi]^T \tag{27}$$

The dynamics of this state are given as:

$$\dot{\boldsymbol{x}}_2(t) = f_2\big(x(t), u_2(t)\big) + \boldsymbol{\Gamma} v(t) \tag{28}$$

where, with $s_\theta = sin\,\theta$, $c_\theta = cos\,\theta$ and $t_\theta = tan\,\theta$:

$$f_2(t) = \begin{bmatrix} 1 & s_\phi t_\theta & c_\phi t_\theta \\ 0 & c_\phi & -s_\phi \\ 0 & \frac{s_\phi}{c_\theta} & \frac{c_\phi}{c_\theta} \end{bmatrix} \begin{bmatrix} p \\ q \\ r \end{bmatrix} \tag{29}$$

and the input vector is given as:

$$\boldsymbol{u_2}(k) = [p \quad q \quad r]_f^T \tag{30}$$

On the other hand, the measurement equation used by the Euler EKF is given as

$$\boldsymbol{z}_2(t) = \boldsymbol{H}_2\boldsymbol{x}_2(t) + w(t) \tag{31}$$

where the measurements vector is given as:

$$\boldsymbol{z}_2 = [\phi \quad \theta \quad \psi] \tag{32}$$

and the measurement matrix is therefore given as

$$H_2 = I_{3x3} \tag{33}$$

Next, simulation results are shown to demonstrate the accuracy of the proposed algorithm.

5. Simulation Result

As a proof of the validity of the presented algorithm, different tests are done. The Three algorithms are compared to estimate the Euler angles. The first method is conducted using the sensors readings directly with the DCM algorithm. The result of this method will be shown as blue solid line. Subsequently, the second method is done using the Rate EKF, which filters the gyros readings, along with the DCM algorithm. The result of this method will be shown using a green solid line. Finally, the third method is done utilizing both the Rate EKF and the Euler EKF with the DCM algorithm to estimate the Euler angles. The result of this method will be shown using a black dashed line. The true Euler angles are shown in the red solid line. Moreover, Monte Carlo tests are presented to prove the reliability of the algorithm in Table 1.

Table 1. The Average of the RMSE of the Monte Carlo tests.

Method	Roll	Pitch	Yaw
DCM + Rate EKF + Euler EKF	0.0859	0.3151	0.0186

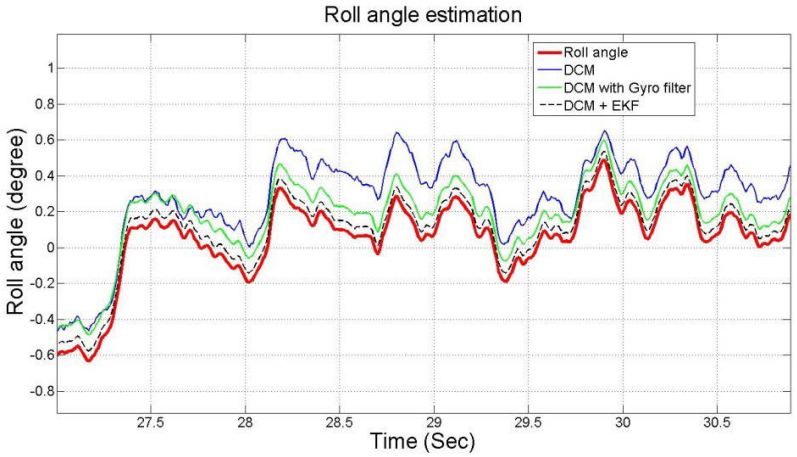

Fig. 4. Roll angle estimation.

6. Conclusion

In this paper, an algorithm was proposed to enhance the estimation of the Euler angles and rates of a quadrotor using the DCM algorithm with two extended Kalman filters. The results show a noticeable improvement in the output of the gyroscope sensors. Additionally, an enhancement of the Euler angles estimates are achieved by using the filtered quadrotor's angular velocity along with the proposed Euler angles EKF. Monte Carlo tests were performed to show the enhancement in the estimation accuracy using the proposed method in comparison to using the DCM approach only or using the DCM approach with the rate EKF only.

References

[1] Jimenez AR, Seco F, Prieto C, Guevara J. A Comparison of Pedestrian Dead-Reckoning Algorithms using a Low-Cost MEMS IMU. 6th IEEE International Symposium on Intelligent Signal Processing, Budapest, Hungary, 2009.
[2] Abdel-Hafez MF. The Autocovariance Least Squares Technique for GPS Measurement Noise Estimation. in IEEE Transactions on Vehicular Technology 2010;59(2):574-588.
[3] Wu F-M, Yang Y-X, Zhang L-P. A new fusion scheme for accuracy enhancement and error modification in GPS/INS tight integrated navigation. Survey Review 2012;44(326):208-214.
[4] Abdel-Hafez MF. Detection of Bias in GPS Satellites' Measurements: A Probability Ratio Test Formulation. IEEE Transactions on Control Systems Technology 2013: DOI: 10.1109/TCST.2013.2267093.
[5] Zhao X. An Improved Adaptive Kalman Filtering Algorithm for Advanced Robot Navigation System based on GPS/INS. International Conference on Mechatronics and Automation, 2011.
[6] Hana S, Wang J. Land Vehicle Navigation with the Integration of GPS and Reduced INS: Performance Improvement with Velocity Aiding. Journal of Navigation 2010;63(1):153-166.
[7] Mahony R, Hamel T, Pflimlin J-M. Nonlinear Complementary Filters on the Special Orthogonal Group. IEEE Transactions on Automatic Control 2008;53(5):1203-1218.
[8] Euston M, Coote P, Mahony R, Kim J, Hamel T. A Complementary Filter for Attitude Estimation of a Fixed-Wing UAV. International Conference on Intelligent Robots and Systems, Nice, France, September 2008.
[9] Baldwin G, Mahony R, Trumpf J, Hamel T, Cheviron T. Complementary filter design on the Special Euclidean group SE (3). In: Proc. of the 2007 European Control Conference, 2007.
[10] Mahony R, Cha SH, Hamel T. A coupled estimation and control analysis for attitude stabilization of mini aerial vehicles. Australiasian Conference on Robotics and Automation, Auckland, New Zealand, 2006.
[11] Phuong NHQ, Kang HJ, Suh YS, Ro YS. A DCM based orientation estimation algorithm with an inertial measurement unit and a magnetic compass. Journal of Universal Computer Science 2009;15(4):859-876.
[12] Al-Omari MAR, Jaradat MA, Jarrah MA. Integrated Simulation Platform for Indoor Quadrotor Applications. In: Proceedings of the 9th International Symposium on Mechatronics and its Applications, Amman, Jordan, April 9-11, 2013.
[13] Bresciani T. Modelling, Identification and Control of a Quadrotor Helicopter. Master Thesis, Department of Automatic Control, Lund University, October 2008.
[14] Bouabdallah S, Murrieri P, Siegwart R. Design and Control of an Indoor Micro Quadrotor. International Conference on Robotics and Automation, New Orleans, Louisiana, 2004.
[15] Johnson E, Turbe M. Modeling, Control, and Flight Testing of a Small Ducted Fan Aircraft. Journal of Guidance, Control and Dynamics 2006;29(4):769-779.
[16] Premerlani W, Bizard P. Direction Cosine Matrix IMU: Theory. http://gentlenav.googlecode.com/files/DCMDraft2.pdf.
[17] Bar-Shalom Y, Li XR, Kirubarajan T. Estimation with Applications to Tracking and Navigation: Theory Algorithms and Software. Hoboken, New Jersey: John Wiley & Sons, Inc.; 2001.